ELSEVIER

Polymer 42 (2001) 6841–6849

polymer

www.elsevier.nl/locate/polymer

A time-of-flight secondary ion mass spectrometry study of sequential polymers with a well-defined segmental length

Lin Li[a,1], Chi-Ming Chan[a,*], Kai-Mo Ng[a], Yuguo Lei[a], Lu-Tao Weng[b]

[a]Department of Chemical Engineering, Advanced Engineering Materials Facility, Hong Kong University of Science and Technology, Clear Water Bay, Kowloon, Hong Kong

[b]Materials Characterization and Preparation Facility, Hong Kong University of Science and Technology, Clear Water Bay, Kowloon, Hong Kong

Received 7 July 2000; received in revised form 1 December 2000; accepted 19 February 2001

Abstract

Two series of sequential polymers (6FBA–C*n* and BA–C*n*) have been synthesized by phase-transfer catalyzed polyetherification of 1,*n*-dibromoalkane ($n = 4, 6, 8, 10, 12, 14$ and 18) with 4,4′-(hexafluoroisopropylidene)diphenol (6FBA) and bisphenol A (BA). The effects of the flexible aliphatic segment length on the structure of secondary ions were investigated. The characteristic secondary positive and negative ions in the time-of-flight secondary ion mass spectrometry (ToF-SIMS) spectra are related to the chemical structures of the sequential BA–C*n* and 6FBA–C*n* polymers. The emission of the characteristic secondary positive and negative ions occurs after cleavage of the C–O bonds of the polymer repeat units. In the ToF-SIMS negative spectra, a series of small peaks separated by 14 amu provides the information about the flexible segment lengths of the repeat units of the BA–C*n* and 6FBA–C*n* polymers and can be used to directly determine the number of the $-CH_2-$ groups, *n*, of the flexible segment. © 2001 Elsevier Science Ltd. All rights reserved.

Keywords: Time-of-flight secondary ion mass spectrometry; Sequential polymers; Flexible segment length

1. Introduction

Time-of-flight secondary ion mass spectrometry (ToF-SIMS) is very useful in surface characterizations of polymers, such as polymer blends [1–4], block and graft copolymers [5–15]. The secondary fragments emitted from a polymer surface have been shown to be related to the surface chemical structure [16,17,27–29]. Moreover, owing to the development of the time-of-flight analyzer, the enhanced capabilities of static ToF-SIMS in sensitivity and mass resolution allow an unambiguous identification of the surface chemical structures, such as chain end groups [18–20], pendant groups [21], repeat units [8,9], polymer chain conformations [22,23], cross linking and branching [6], and segment length distribution [15,24]. In particular, ToF-SIMS can provide structural information in both positive and negative spectra. However, up until now, the formation mechanisms of the secondary fragments under ion beam bombardment are still not fully established [25–29]. It is difficult to understand the formation and emission processes of large fragment ions from polymer surfaces. Furthermore, without a good understanding of the relationship between the secondary ion structures and polymer chain structures, the applications of ToF-SIMS to problems of polymer identification and quantification are limited. The analysis and interpretation of the ToF-SIMS spectra of the sequential BA–C*n* and 6FBA–C*n* polymers with well-defined segment lengths may provide a good understanding of the effects of the surface chemical structure and the flexible segment length on the structures of the characteristic secondary fragment ions.

2. Experimental section

2.1. Materials

1,4-Dibromobutane, 1,6-dibromohexane, 1,8-dibromooctane, 1,10-dibromodecane, 1,12-dibromododecane, tetrabutylammonium hydrogen sulphate, 1,2-dichlorobenzene and Bisphenol-A (Aldrich or Acros) were used as received. 4,4′-(hexafluoroisopropylidene)diphenol from Fluorochem was recrystallized from hot toluene. 1,14-dibromotetradecane and 1,18-dibromooctadecane were prepared by a literature method [30].

---

[*] Corresponding author. Tel./fax: +852-2358-7125.
E-mail address: kecmchan@ust.hk (C.-M. Chan).

[1] Present address: State Key Laboratory of Polymer Physics and Chemistry, Center for Molecular Science, Institute of Chemistry, Chinese Academy of Science, Beijing 100080, People's Republic of China.

PII: S0032-3861(01)00153-7

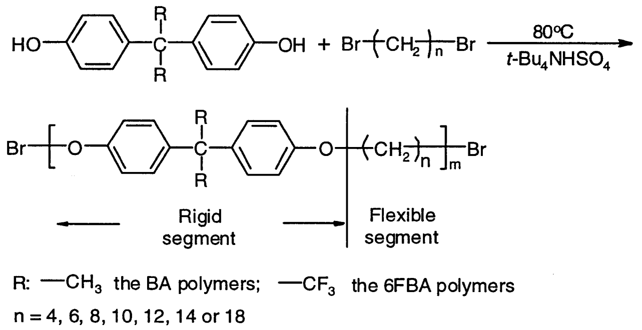

Scheme 1.

2.2. Polymer preparation

The BA–C*n* and 6FBA–C*n* sequential polymers were synthesized by condensation polymerization using BA or 6FBA and 1,*n*-dibromoalkane ($n = 4, 6, 8, 10, 12, 14$ and 18) with a catalytic amount of phase transfer agent *tetra*-butylammonium hydrogen sulphate. The synthesis is described in Scheme 1. (Reaction and general structures of the BA–C*n* and 6FBA–C*n* sequential polymers.) A very small excessive amount of 1,*n*-dibromoalkane was used in order to keep Br atom as the end-group.

2.3. Characterization methods

Glass transition temperature (T_g) was determined by TA 2910. The molecular weights were determined by gel permeation chromatography, using chloroform as solvent and poly(ethylene glycol) as standard. The results are given in Table 1. Surface analyses were performed by a Physical Electronics PHI 7200 ToF-SIMS spectrometer. The high-resolution mass spectra were obtained by ToF-SIMS using a Cs^+ primary ion source operating at 8 keV. The total ion dose was lower than 4×10^{11} ions/cm^2. Thin films of the BA–C*n* and 6FBA–C*n* sequential polymers were prepared by solution spin casting on silicon wafers. The solvents used for the BA–C*n* and 6FBA–C*n* sequential polymers were chloroform and tetrahydrofuran, respectively. Three positive and three negative spectra were taken for each sample.

Table 1
Results of the characterizations of the BA–C*n* and 6FBA–C*n* sequential polymers

Samples	T_g (°C)	T_m (°C)	$\bar{M}_w \times 10^3$	$\bar{M}_w/\bar{M}_n$
BA–C4	50.9	186.0	21.1	2.38
BA–C6	31.0	97.4	24.1	1.67
BA–C8	6.3	84.3	9.5	1.68
BA–C10	0.3	88.5	13.8	2.01
BA–C12	−5.9	88.3	16.2	2.05
BA–C14	−6.7	86.9	29.6	3.52
BA–C18	−4.1	81.8	28.6	3.49
6FBA–C4	60.4		17.6	1.79
6FBA–C6	46.4		24.1	1.88
6FBA–C8	27.7		8.0	1.52
6FBA–C10	13.1		11.1	2.04
6FBA–C12	5.0		21.5	1.92
6FBA–C14	13.0		38.0	1.87
6FBA–C18	4.1		91.2	2.30

3. Results and discussion

The ToF-SIMS spectra of the BA–C*n* and 6FBA–C*n* polymers can be divided into two regions: the low mass region ($m/z = 0$–300 amu) and the high mass region ($m/z = 300$–500 amu). In the low mass range of the positive and negative ToF-SIMS spectra, the characteristic secondary ions can provide some molecular and structural information of the BA–C*n* and 6FBA–C*n* polymer surfaces. For example, the peak at $m/z = 69$ amu is produced from the $-CF_3$ side group of the 6FBA–C*n* polymers. The spectra of the high mass range consist of large fragments that are related to the repeat unit and end-groups, forming a unique series pattern for a given segment length of the repeat unit of the BA–C*n* and 6FBA–C*n* sequential polymers.

3.1. ToF-SIMS positive spectra

3.1.1. Low mass region ($m/z = 0$–300 amu)

ToF-SIMS positive spectra are presented in Fig. 1a–d for the BA–C4, BA–C6, BA–C8 and BA–C10, respectively. Fig. 2a and b is for the 6FBA–C6 and 6FBA–C8, respectively. The positive BA–C*n* and 6FBA–C*n* spectra comprise a series of aliphatic hydrocarbon and aromatic hydrocarbon fragments. The aliphatic hydrocarbon positive ions ($-C_2H_3^+$, $-C_2H_5^+$, $-C_3H_5^+$, $-C_3H_7^+$, $-C_4H_7^+$, $-C_4H_9^+$ and $-C_5H_9^+$ at $m/z = 27$, 29, 41, 43, 55, 57 and 69 amu, respectively) are produced from the flexible aliphatic segments of the repeat units of the BA–C*n* and 6FBA–C*n* sequential polymers. A comparison between Figs. 1 and 2 show the aliphatic hydrocarbon positive ions of the BA–C*n* and 6FBA–C*n* polymers are very similar to each other. These results suggest that the aliphatic hydrocarbon positive ions emitted from the same flexible segments of the BA–C*n* and 6FBA–C*n* polymers are produced by a similar fragmentation pathway. The influence of the structure of the aromatic rigid segment and its side groups on the fragmentation of the aliphatic flexible segment is qualitatively very small. However, the intensities of some of the aliphatic hydrocarbon peaks show significant changes as the flexible segment length of the BA–C*n* and 6FBA–C*n* sequential polymers increases. For example, the normalized intensity of peaks (I_n) at $m/z = 29$, 43, and 57 amu increases as the flexible aliphatic segmental length increases, as shown in Fig. 3. The normalized intensity is defined as

$$I_n = \frac{I}{I_T}, \qquad (1)$$

where I is the measured peak intensity and I_T is the total intensity of the positive ions in the mass range $m/z = 0$–500 amu. As shown in Fig. 3a and b, the normalized intensities of the

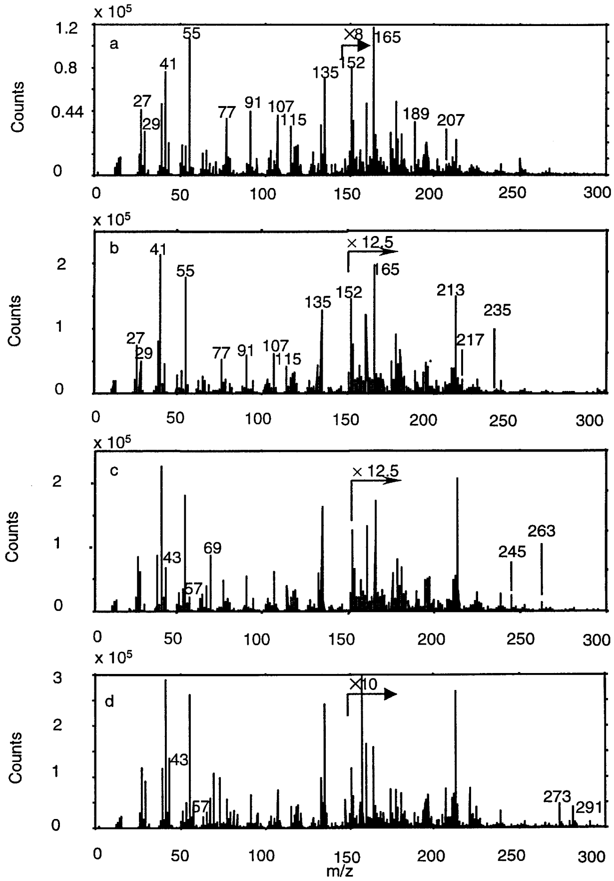

Fig. 1. Positive ToF-SIMS spectra of the BA–C*n* polymers in the range *m*/*z* = 0–300 amu: (a) BA–C4, (b) BA–C6, (c) BA–C8, and (d) BA–C10.

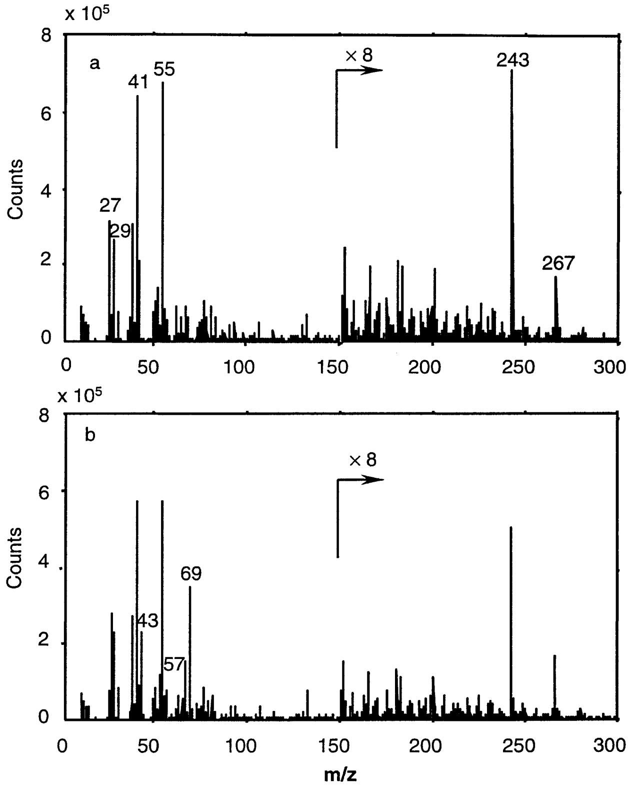

Fig. 2. Positive ToF-SIMS spectra of the 6FBA–C*n* polymers in the range *m*/*z* = 0–300 amu: (a) 6FBA–C6, and (b) 6FBA–C8.

characteristic peaks increase linearly with the length of the flexible segment. These results indicate that the aromatic rigid segment and its side groups, $-CH_3$ and $-CF_3$, have almost no effect on the fragmentation of the saturated flexible aliphatic segment.

The structural difference between the BA–C*n* and 6FBA–C*n* sequential polymers lies in the side groups of the rigid segments. The side groups of the BA–C*n* and 6FBA–C*n* sequential polymers are $-CH_3$ and $-CF_3$, respectively, as shown in Scheme 1. This difference means the characteristic positive ions of the rigid segments of the BA–C*n* and 6FBA–C*n* polymers lie in different mass ranges. The characteristic positive ions at $m/z = 107$, 135, and 213 amu ($C_7H_7O^+$, $C_9H_{11}O^+$ and $C_{14}H_{13}O_2^+$, respectively), are emitted from the rigid segments of the BA–C*n* polymers. While the characteristic positive ions at $m/z = 243$ and 267 amu ($C_9F_6H_5O^+$ and $C_{14}F_3H_{10}O_2^+$, respectively) are emitted from the rigid segments of the 6FBA–C*n* polymers. The essential structures of $C_9H_{11}O^+$ and $C_{14}H_{13}O_2^+$ from the BA–C*n* polymers are the same as those of $C_9F_6H_5O^+$ and $C_{14}F_3H_{10}O_2^+$ emitted from the 6FBA–C*n* polymers, as shown in Scheme 2. (Characteristic positive ion structures of the BA–C*n* and 6FBA–C*n* polymers.)

The difference in the side groups and flexible segment length does not appear to have any significant effect on the fragmentation of the rigid segments. The other aromatic

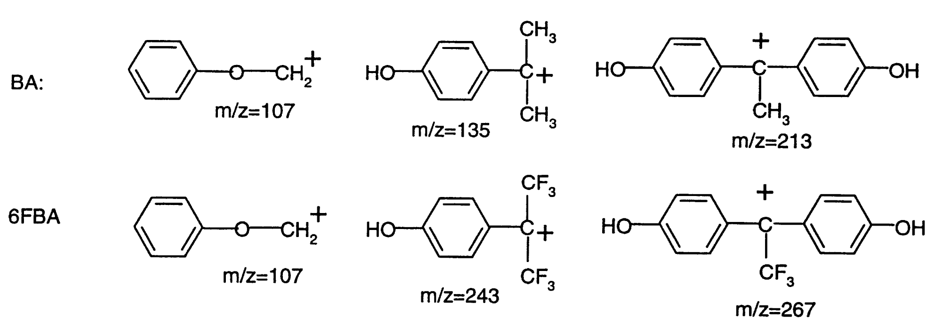

Scheme 2.

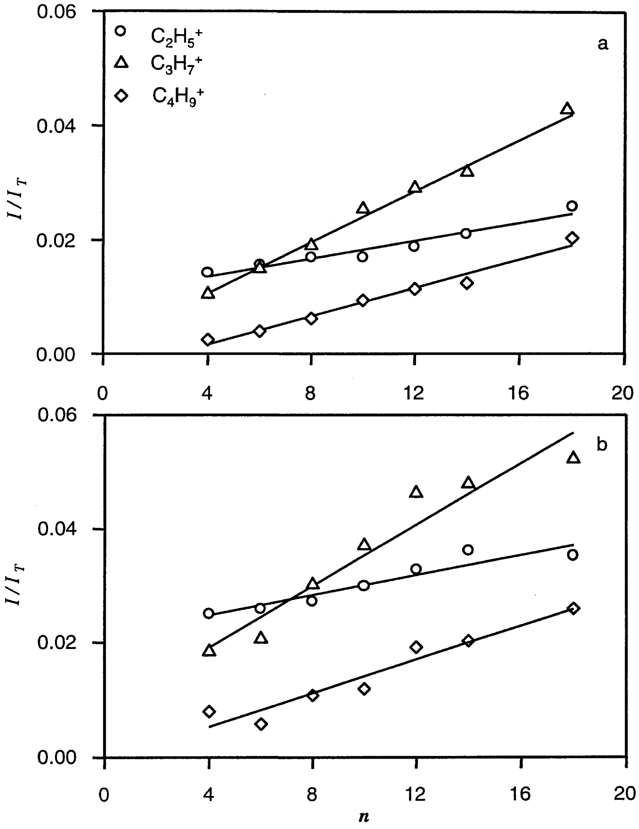

Fig. 3. The normalized intensities of the characteristic positive saturated aliphatic hydrocarbon ions vs. the flexible aliphatic segment length: (a) BA–C*n* polymers, and (b) 6FBA–C*n* polymers.

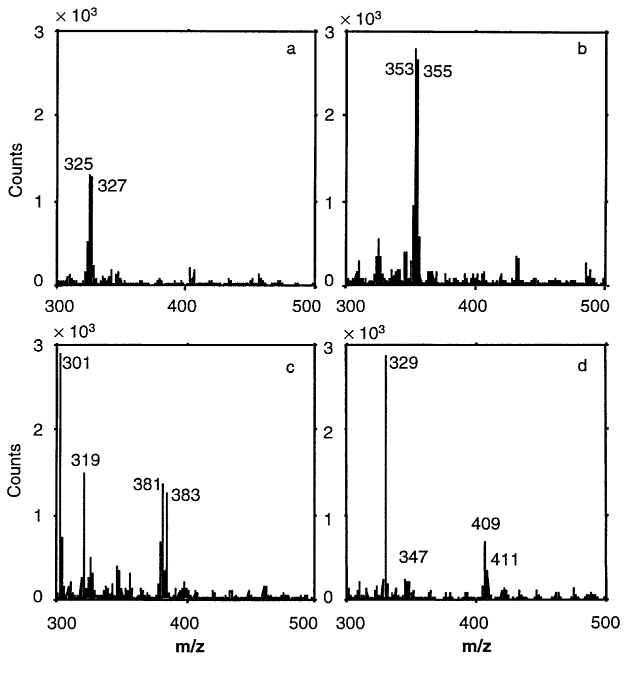

Fig. 4. Positive ToF-SIMS spectra of the BA–C*n* polymers in the range *m*/*z* = 300–500: (a) BA–C8, (b) BA–C10, (c) BA–C12, and (d) BA–C14.

Table 2
Sequential ions of the BA–C*n* polymers

Sequential ions	*n*	BA (*m*/*z*)	
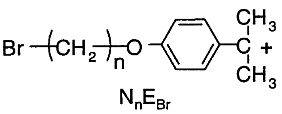 N$_n$E$_{Br}$	8	325	327
	10	353	355
	12	381	383
	14	409	411
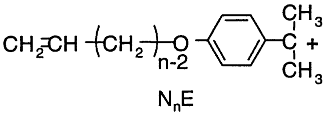 N$_n$E	4	189	
	6	217	
	10	273	
	8	245	
	12	301	
	14	329	
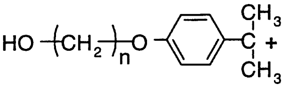 N$_n$O	4	207	
	6	235	
	10	291	
	8	263	
	12	319	
	14	347	

ions, $-C_6H_5^+$, $-C_7H_7^+$, $-C_9H_7^+$, $-C_{12}H_8^+$, and$-C_{13}H_9^+$ at *m*/*z* = 77, 91, 115, 152 and 165 amu, respectively, are also emitted from the rigid segments of the repeat units of the BA–C*n* and 6FBA–C*n* (cf. Figs. 1 and 2). The structures of these aromatic ions are the same as those of the positive ions emitted by polystyrene.

3.1.2. High mass region m/z = 300–500 amu

It is worth noting the high-mass secondary ions can provide more information about the structure of the repeat units and end-groups. Fig. 4 shows the high mass ToF-SIMS spectra for the polymers BA–C8, BA–C10, BA–C12 and BA–C14. Several sequential fragments are observed and their structures are given in Table 2. Three series of fragments are identified. The fragments from the same series differ from each other by 28 amu (C_2H_4). These sequential fragments can easily be assigned based on the molecular structure of the BA–C*n* polymers and are listed as follows:

1. The fragments containing bromine are directly related to the end-groups. For example, the characteristic end-group ions at *m*/*z* = 325 and 327 amu of BA–C8, N_8E_{Br}, as shown in Table 2 (cf. Fig. 4a) are composed of the end-group ($-^{79}Br$ or $-^{81}Br$), the flexible segment ($(-CH_2-)_8$), and a part of the rigid segment ($-C_9H_{10}O$) of the first repeat unit attached to the end-group. The end-group ions at *m*/*z* = 353 and 355 amu of BA–C10, $N_{10}E_{Br}$, have a similar structure to that of N_8E_{Br}. As the length of the flexible segment increases the end-group ions at *m*/*z* = 381 and 383 amu are observed for BA–C12 and those at *m*/*z* = 409 and 411 amu are observed for BA–C14. The only difference between these sequential end-group ions, N_nE_{Br}, is the length of the flexible segment. Consequently, these sequential N_nE_{Br} ions can

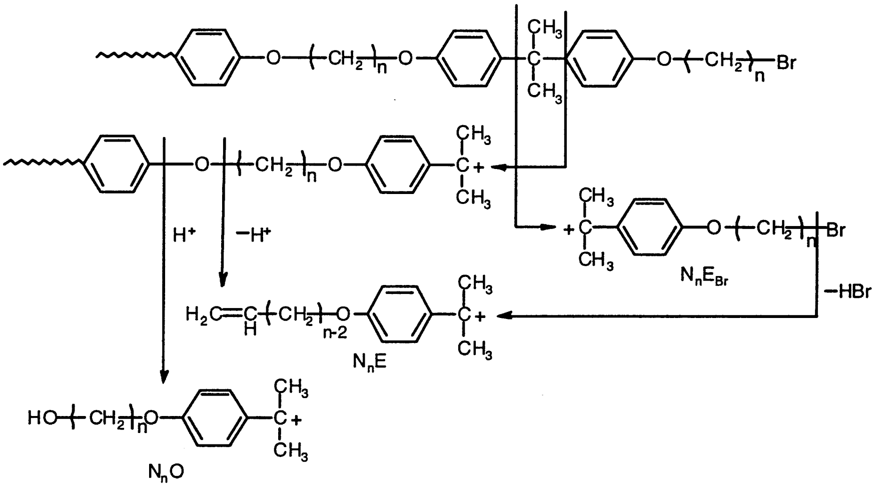

Scheme 3.

only be emitted directly from the first repeat unit by breaking the C–C bond of the rigid segments.

2. The sequential ions, N_nE, are produced through a rearrangement of the sequential N_nE_{Br} ions by elimination of HBr. The sequential N_nE ions of BA–C12 at $m/z =$ 301 amu and of BA–C14 at $m/z = 329$ are typical examples. These N_nE ions may also be emitted from the polymer surface by a direct scission at the main chain of the C–C and C–O bonds of the rigid segments.

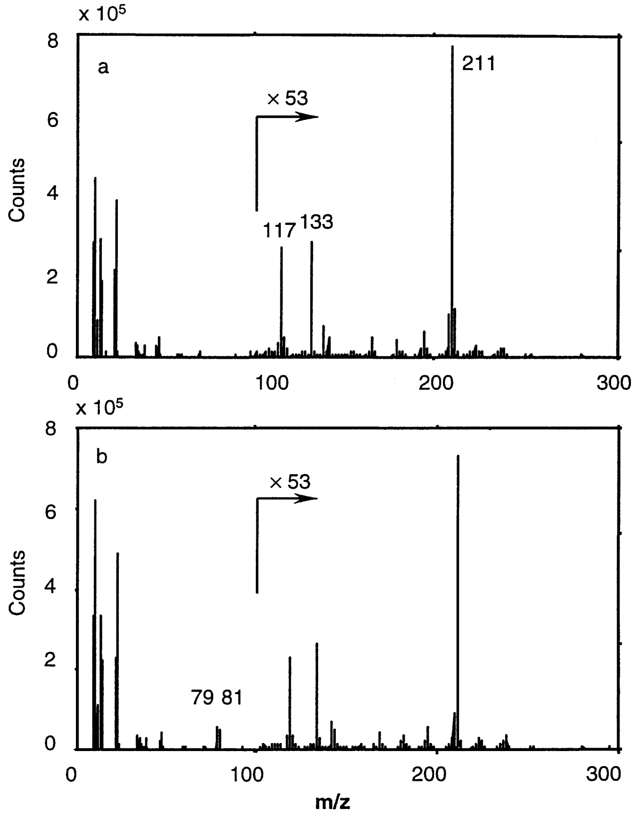

Fig. 5. Negative ToF-SIMS spectra of the BA–C*n* polymers in the range m/z = 0–300: (a) BA–C6, and (b) BA–C8.

3. In the case of the fragmentation by the direct scission of the polymer main chains, sequential ions, N_nO, the structure of which is shown in Table 2, can also be formed.

Scheme 3 (end-group scission of the BA–C*n* polymers) presents the proposed fragmentation process of these characteristic sequential ions — N_nE_{Br}, N_nE, and N_nO. Clearly, the formation of the sequential ions, N_nE_{Br}, N_nE, and N_nO, may be attributed to the stability of the cationic tertiary carbon ions. The influence of the flexible aliphatic segment length on the fragmentation of the rigid segment of the first repeat unit is very weak. The formation of the sequential secondary ions, emitted from the first repeat unit of the BA–C*n* polymers, suggests that the stability of the secondary ions play an important role in the ToF-SIMS process. The positive ToF-SIMS spectra of the 6FBA–C*n* polymers in the range $m/z = 300$–500 amu show similar result with those of the BA–C*n* polymers.

3.2. ToF-SIMS negative spectra

3.2.1. Low mass region ($m/z = 0$–300 amu)

The negative ToF-SIMS spectra of the BA–C*n* and 6FBA–C*n* polymers are shown in Figs. 5 and 6, respectively. Except for the different intensities of the end-group peaks, $-^{79}Br^-$and $-^{81}Br^-$ at $m/z = 79$ and 81 amu, the spectra of BA–C6 and BA–C8 are very similar. The different intensities of the end-group peaks are mainly produced by the difference in molecular weight between BA–C6 and BA–C8. The BA–C8 polymer has the lowest molecular weight of all BA–C*n* polymers. Therefore, the intensities of the end-groups, $-^{79}Br^-$ and $-^{81}Br^-$ of the BA–C8 polymer are very high. To provide stronger evidence that the difference in the Br signal is caused by the difference in the molecular weight, negative ToF-SIMS spectra for BA–C8 polymers with different molecular weights ($\bar{M}_w$ = 9, 500, 22, 920, and 48, 770) were obtained and the results are shown in Fig. 7. It is clearly shown that the Br signal is the highest for the polymer with the lowest molecular

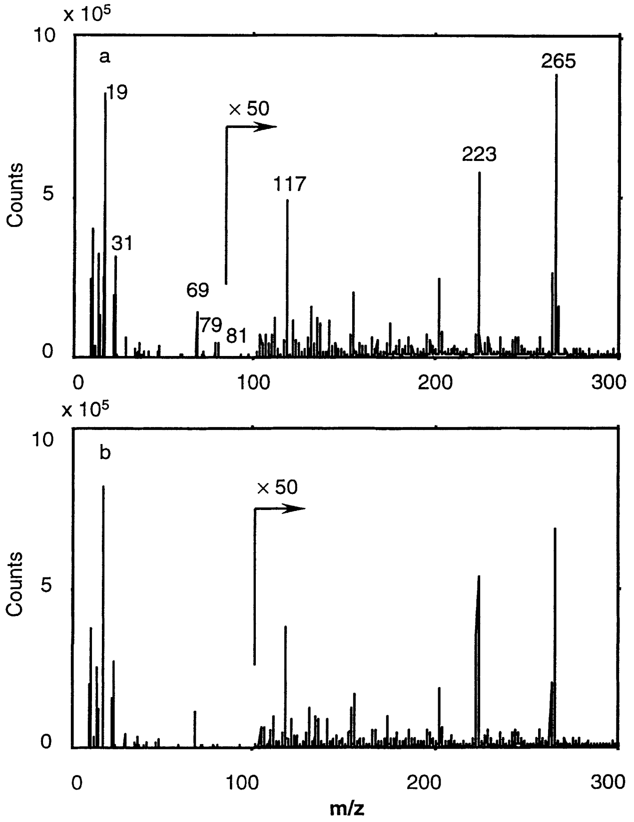

Fig. 6. Negative ToF-SIMS spectra of the 6FBA–C*n* polymers in the range *m*/*z* = 0–300: (a) 6FBA–C6, and (b) 6FBA–C8.

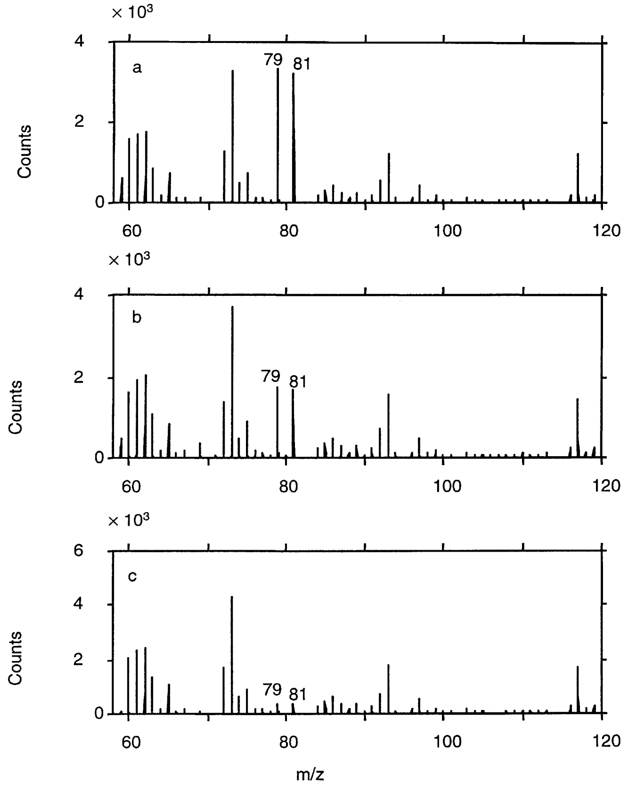

Fig. 7. Negative ToF-SIMS spectra of three BA–C8 polymers with different molecular weights: (a) $\bar{M}_w = 9500$, (b) $\bar{M}_w = 22{,}920$, and (c) $\bar{M}_w = 48{,}770$.

weight. It is important to point out that the Br concentration is not only dependent on the molecular weight but also the crystallinity of the polymer [31]. These three samples analyzed right after they were prepared to make sure that they did not have a significant amount of crystallinity. The similarity in the negative-SIMS spectra indicates that the influence of the flexible aliphatic segment length on the structures of the characteristic negative secondary ions in the range *m*/*z* = 0–300 amu is very similar for both the BA–C*n* and 6FBA–C*n* polymers.

One key difference between the spectra of the BA–C*n* and 6FBA–C*n* polymers is that the peaks at *m*/*z* = 19 amu ($-F^-$), 31 amu ($-CF^-$) and 69 amu ($-CF_3^-$), etc. include the $-CF_3$ side groups, and portions of these side groups, of the rigid segments of the 6FBA–C*n* polymers. Another difference is the spectra of the BA–C*n* polymers are dominated by the peaks at *m*/*z* = 117, 133, and 211 amu, while the spectra of the 6FBA–C*n* polymers are dominated by the peaks at *m*/*z* = 117, 223, and 265 amu. The structures of the characteristic negative ions with these masses are shown in Scheme 4. (Structures of the characteristic negative ions of the BA–C*n* and 6FBA–C*n* polymers.)

The basic structures of these characteristic negative ions emitted from the rigid segments of the BA–C*n* and 6FBA–C*n* polymers are the same. These results are also in agreement with those results obtained from the positive ToF-SIMS spectra of the BA–C*n* and 6FBA–C*n* polymers. It may be concluded that those characteristic positive and negative secondary ions with the structures shown in Scheme 5 (structures of some stable secondary ions where

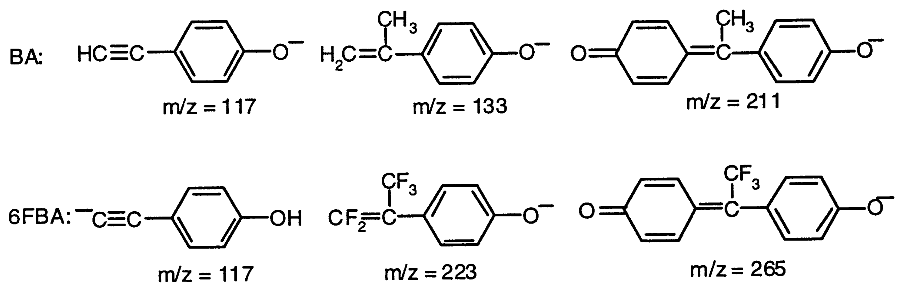

Scheme 4.

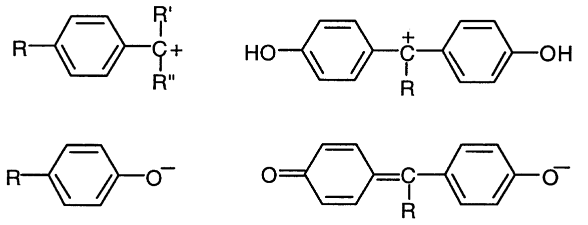

Scheme 5.

–R, –R′ and –R″ are the same or different functional groups, e.g. –OH, –CH_3, –CF_3 and –$O(CH_2)_nH$) are stable, and therefore, easily observed in the ToF-SIMS spectra. Thus, the formation of the characteristic secondary ions may be depended on its stability.

3.2.2. High mass region (m/z = 300–500 amu)

The sequential BA–C*n* polymers with varying length of flexible aliphatic segment, $n = 4$, 6, 8, 10, 12, 14 and 18, respectively, are presented in Fig. 8. The important fragments of the BA–C*n* polymers at $m/z = 281$, 309, 337, 365, 393, 421, and 477 amu are directly emitted by cleaving the C–O bond between the oxygen and the aliphatic carbon of the BA–C*n* polymer. The structures of the characteristic secondary ions are shown in Table 3. The peaks for characteristic negative fragments, [M − H], at $m/z = 281$, 309, 337, 365, 393, 421 and 477 amu correspond to the loss of an hydrogen atom from the repeat units, [M], of BA–C4, BA–C6, BA–C8, BA–C10, BA–C12, BA–C14 and BA–C18, respectively. A random copolymer of BA–C8 and BA–C14 was prepared to confirm these peaks in the negative ToF-SIMS spectra. The negative spectrum of this random copolymer is shown in Fig. 8h. The important negative fragments of the BA–C8/BA–C14 random copolymer films occur at $m/z = 337$ and 421 amu, and are the same as the fragment at $m/z = 337$ amu for the BA–C8 polymer and the fragment at $m/z = 421$ amu for the BA–C14 polymer. These results show the potential usefulness of ToF-SIMS analyses in the direct identification of polymeric materials, even when the polymers have very similar structures.

Furthermore, the observation of the peaks, [M + OH], at $m/z = 299$, 327, 355, 383, 411, 439, and 495 amu in the spectra, as shown in Fig. 8a–g, suggests the cleavage also occurs at the C–O bond between the oxygen and the aromatic carbon of the BA–C*n* polymers. Due to the use

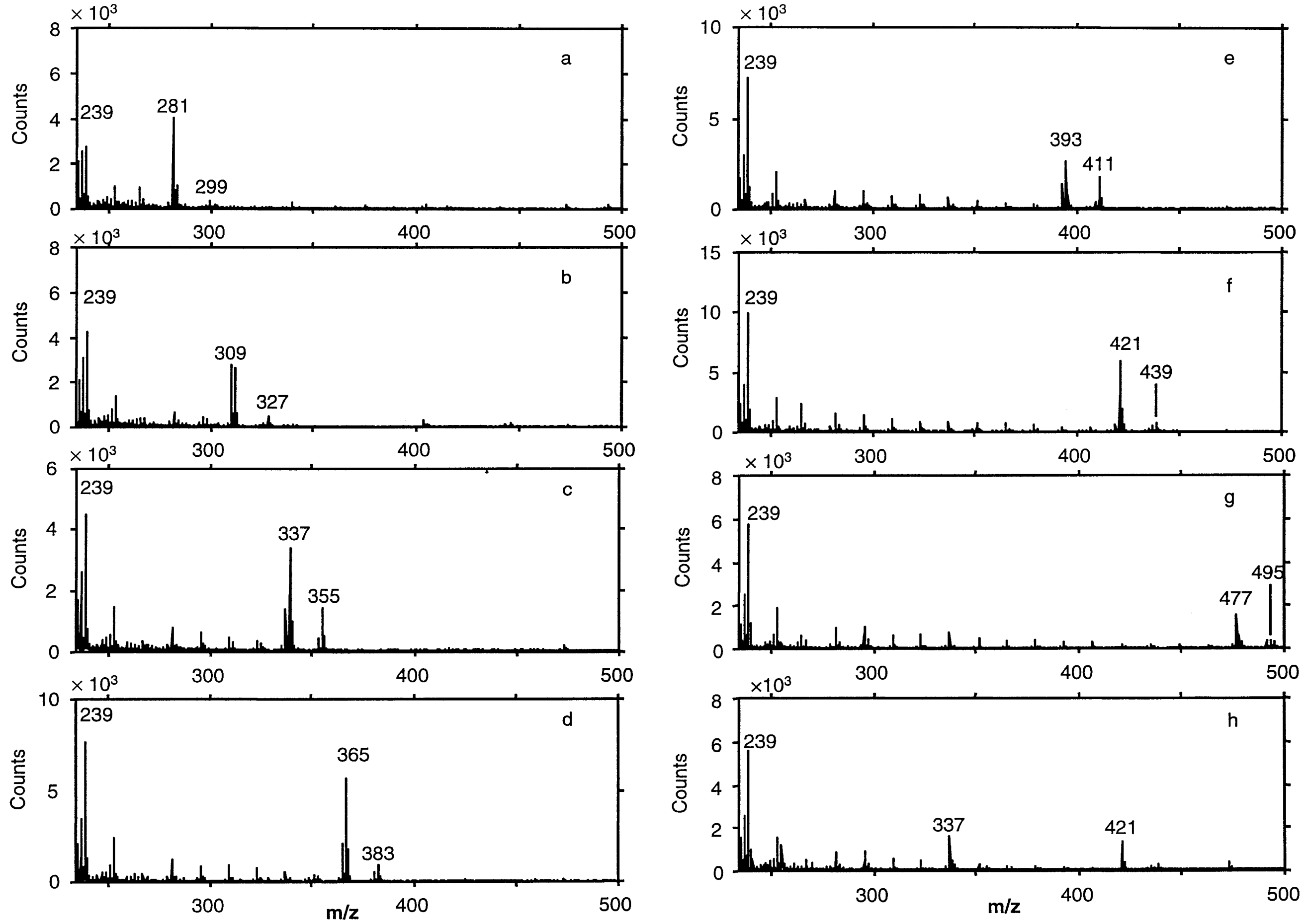

Fig. 8. Negative ToF-SIMS spectra for the BA–C*n* polymers: (a) BA–C4, (b) BA–C6, (c) BA–C8, (d) BA–C10, (e) BA–C12, (f) BA–C14, (g) BA–C18, and (h) BA–C8/BA–C14 random copolymer.

Table 3
Structures of the negative ions and the repeat units of the BA–C*n* polymers

Structures	*n*	*m*/*z*
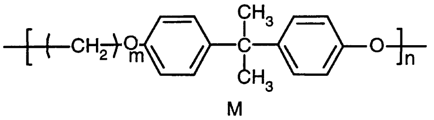 M	4	282
	6	310
	8	338
	10	366
	12	394
	14	422
	18	478
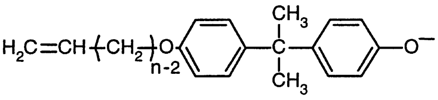 M - H	4	281
	6	309
	8	337
	10	365
	12	393
	14	421
	18	477
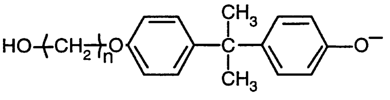 M+OH	4	299
	6	327
	8	355
	10	383
	12	411
	14	439
	18	495

of a small excess of the 1,*n*-dibromoalkane during the polymerization, only bromine is present at both ends of the BA–C*n* polymers. Therefore, all the [M + OH] fragments are emitted by internal scission of the BA–C*n* polymer main chains. The high intensities of the [M − H] and the low intensities of the [M + OH] peaks indicate that the cleavage of the C–O bond between the oxygen and the aliphatic carbon of the BA–C*n* polymer is favorable. The observation of the peaks associated with [M − H] fragments at $m/z = 337$ and 421 amu in the negative spectrum of the BA–C8/BA–C14 random copolymer also suggests the influence of the flexible segment length on the cleavage of the O–C (aliphatic) bond is very small.

The sequential small peaks, for example BA–C14 polymer shown in Fig. 8f, at $m/z = 239$, 253, 267, 281, 295, 309, 323, 337, 351, 365, 379, 393, and 407 amu (each peak is separated by 14 amu from the ones above and below it) are produced by direct scission of the C–C bonds of the flexible aliphatic segment of the repeat unit. These fragments may also be produced by the rearrangement of the [M − H] fragments at $m/z = 421$ amu of the BA–14, during secondary ion emission. The number of $-CH_2-$ groups, *n*, can be precisely determined using these sequential peaks of the negative secondary ions. It is easier to determine the number of $-CH_2-$ groups using ToF-SIMS comparing with that using other techniques, such as NMR. The fragmentation of the 6FBA–C*n* polymers with different flexible segment lengths is very similar to that of the BA–C*n* polymers. The peaks for the repeat units and the sequential small peaks separated by 14 amu can also be observed in ToF-SIMS negative spectra of the 6FBA–C*n* polymers. A possible fragmentation pathway through the direct scission of the BA–C*n* polymer main chains is illustrated in Scheme 6 (a possible fragmentation pathway of the BA–C4 polymer under low-energy ion beam bombardment) for the BA–C4 polymer films under the bombardment of a primary Cs^+ ion beam.

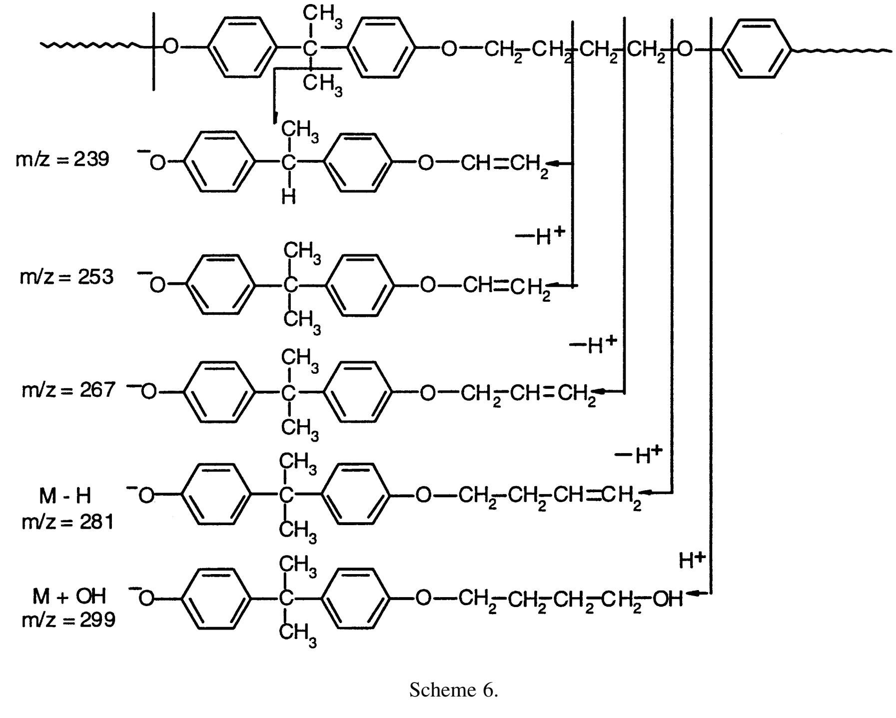

Scheme 6.

4. Conclusions

ToF-SIMS has been applied to study the surface of the BA–C*n* and 6FBA–C*n* polymers with well-defined flexible aliphatic segment lengths ($n = 4$, 6, 8, 10, 12, 14 and 18). The results suggest that the influence of the flexible aliphatic segment lengths on the fragmentation of the rigid segment is limited. Similar fragmentation pathways can be assumed for the characteristic secondary ions generated from the surface of the BA–C*n* and 6FBA–C*n* polymers. The stability of secondary ions plays an important role during the fragmentation of polymer chain. The structures of the characteristic secondary ions are directly related to the molecular structures of the BA–C*n* and 6FBA–C*n* polymers. The end-groups, pendent groups, repeat units and the number of $-CH_2-$ groups of the BA–C*n* and 6FBA–C*n* polymers can be easily detected in ToF-SIMS analyses. These results indicate ToF-SIMS can be used to directly identify polymers with very similar structures. It is also suggested that the detailed structures of polymer chains, such as the number of $-CH_2-$ groups can be precisely determined using ToF-SIMS.

Acknowledgements

This work was supported by the Hong Kong Government Research Grants Council under grant number HKUST 9123/97P.

References

[1] Affrossman S, Bertrand P, Hartshorne M, Kiff T, Leonard D, Pethrich RA, Richards RW. Macromolecules 1996;29:5432.
[2] Lhoest JB, Bertrand P, Weng LT, Dewez JL. Macromolecules 1995;28:4631.
[3] Bhatia QS, Burrell MC. Surf Interface Anal 1990;15:388.
[4] Chilkoti A, Castner DG, Ratner BD, Briggs D. J Vac Sci Technol A 1990;8:2274.
[5] Castner DG, Ratner BD. Surf Interface Anal 1990;15:479.
[6] Briggs D. Surf Interface Anal 1990;15:734.
[7] Lub J, van Vroonhoven FCBM, van Leyen D, Benninghoven A. J Polym Sci, Polym Phys Ed 1989;27:2071.
[8] Newman JG, Carlson BA, Michael RS, Moulder JF, Holt TH. Static SIMS handbook of polymer analysis. Perkin–Elmer Corporation Edition; 1991.
[9] Briggs D, Brown A, Vickerman JC. Handbook static secondary ion mass spectrometry (SIMS). Chichester: Wiley, 1989.
[10] Galuska AA. Surf Interface Anal 1997;25:1.
[11] Bhatia QS, Burrell MC. Polymer 1991;32:1948.
[12] Chen X, Lee HF, Gardella Jr. JA. Macromolecules 1993;26:3778.
[13] Chen X, Gardella Jr. JA. Macromolecules 1994;27:3363.
[14] Zhuang HZ, Gardella Jr. AJ. Macromolecules 1997;30:3632.
[15] Zhuang HZ, Gardella Jr. AJ, Hercules DM. Macromolecules 1997;30:1153.
[16] Briggs D. Surface analysis of polymers by XPS and static SIMS. Cambridge: Cambridge University Press, 1998.
[17] Chan CM. Polymer surface modification and characterization. New York: Hanser, 1994.
[18] Fowler DE, Johnson D, Vanleyen D, Benninghoven A. Surf Interface Anal 1991;17:125.
[19] Galuska AA. Surf Interface Anal 1997;25:790.
[20] Vanden Eynde X, Bertrand P. Surf Interface Anal 1998;26:579.
[21] Casnter DG, Ratner BD. Surf Interface Anal 1990;16:479.
[22] Zimmerman PA, Hercules DM. Appl Spectrosc 1994;48:620.
[23] Vanden Eynde X, Weng LT, Bertrand P. Surf Interface Anal 1997;25:41.
[24] Chen X, Gardella Jr. AJ, Ho T, Wynne KJ. Macromolecules 1995;28:1635.
[25] Benninghoven A, Lange W, Jirikowsky M, Holtkamp D. Surf Sci 1982;123:721.
[26] Leggett GJ, Vickerman JC. Int J Mass Spectrom Ion Processes 1992;122:281.
[27] van Ooij WJ, Brinkhuis RHG. Surf Interface Anal 1988;11:430.
[28] Chilkoti A, Ratner BD, Briggs D. Surf Interface Anal 1992;18:604.
[29] Leggett GJ, Vickerman JC. Surf Interface Anal 1992;18:637.
[30] Vial H, Calas M, Ancelin M-L, Giral L. PCT Int Appl WO 9804252.
[31] Li L, Ng K-M, Chan C-M, Feng J-Y, Zeng X-M, Weng L-T. Macromolecules 2000;33:5588.